Novel animal model for ventricular ejection fraction measured by MRI

Josefino B. Tunac, PhD[1], Robert Knight, PhD[2] and Frederick Valeriote, PhD[2]
[1]*Arterez, Inc,*
[2]*Henry Ford Health System*

***Highlights**:*

- First to demonstrate ventricular ejection fraction (VEF) per cine magnetic resonance imaging (MRI) in wild non-surgical or non-genetic mouse, the Tunac Arterial Plaque (TAP) model
- TAP model involved feeding the mouse with high fat diet and treatment with the ubiquitous environmental pollutant, PCB, which in combo created inflammation and produced arterial plaques.
- Disruption of arterial endothelial glycocalyx triggered plaque formation, which weakened the integrity of cardiac cells (myocytes) and resulted in a reduced % VEF.
- Plaque formation in aortal arch was confirmed by MRI, which involved multiple contrast weightings (e.g., T1, T2, and proton density).

INTRODUCTION

Ejection fraction and heart failure

An ejection fraction (EF) is the volume of blood ejected from the left ventricle with each heartbeat, which is used as a measure of the pumping efficiency of the heart. EF is calculated by dividing the volume of blood pumped by the volume collected at the end of diastolic filling. A reduction in EF is a sign of heart failure (HF), which can be subdivided into 3 categories:

1. normal or preserved ejection fraction (HFpEF): ≥50% – referred to as diastolic heart failure where the heart muscle contracts normally but the ventricles do not relax during ventricular filling.
2. moderately reduced: 40–49%] (HFmrEF)
3. reduced ejection fraction (HFrEF): <40% – referred to as systolic heart failure where the heart muscle does not contract effectively resulting in less oxygen-rich blood pumped out to the body

HF (aka, CHF, or chronic heart failure) is a global pandemic affecting at least 26 million people worldwide and is increasing in prevalence (2014. ESC Heart Failure 1:4–25) affecting approximately 1 - 2% of adult population. Of the estimated 5 million patients in the US diagnosed with HF, approximately 50% are preserved ejection fraction (HFpEF) and its prevalence is increasing by about 1% annually *(2019. Circ Res. 124:1598-1617)* relative to that of reduced ejection fraction (HFrEF) incidence (2016. Circulation 134:73-90). HF accounts for more than 80 000 deaths annually in the US and an estimated $69.8 billion in annual health care spending by 2030 *(2020. Circulation 141: e139-e596*).

HF is a multifactorial, systemic disease triggered by damaged heart muscle (myocardium), followed by the activation of structural, neurohumoral, cellular, and molecular mechanisms to maintain physiological functioning (2011. *Eur Heart J. 32:670–679)*. Currently, there is no

effective treatments for HfpEF, which is due to the lack of pre-clinical models to allow extensive imaging and therapeutic evaluation *(2017. Circ Res 120: 1243–1245)*

In this regard, there is a need for a murine model of EF to evaluate novel therapies, particularly the left ventricular ejection fraction (LVEF), which is a strong independent predictor of cardiovascular morbidity and death *(1999. Circulation. 1035–1042).* Currently, a typical animal model involves a genetically modified mouse lacking osteopontin, treated with aldosterone and 1% sodium chloride (NaCl) to induce blood pressure elevation, cardiac hypertrophy, and fibrosis *(2004. Am J Hypertens 17:188–93).* Another option is a mouse with coronary arteries surgically narrowed to mimic ischemic cardiomyopathy (ICM) as a means of triggering myocardial infarction (MI). For example, a C57BL/6 wildtype (WT) mouse surgical occluded at the left anterior descending artery (LAD) creating MI then EF evaluated by MRI after 4 weeks *(2006. FASEB J. 20:956–958).*

The disruption of the endothelial glycocalyx is the upstream component of EF, which trigger coronary plaques and contribute to myocyte stiffness and reduced EF volume particularly in the left ventricle *(2018. Eur Heart J 39: 3439–3450).* Meanwhile, MI is the most visible symptom, which develop HF and a sequalae of downstream diseases including a cardio-renal syndrome, which is the endpoint of HF (Fig.).

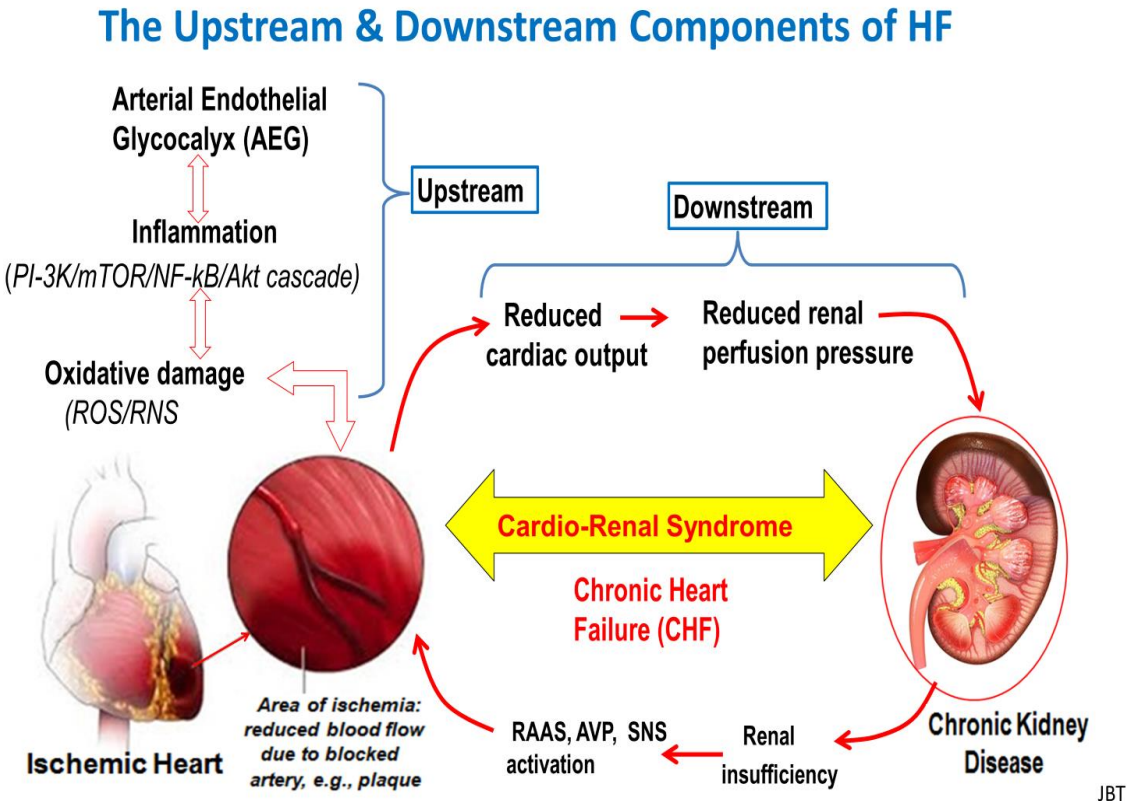

Figure 1. Disrruption of the arterial endothelial glycocalyx triggers a cascade of diseases including the cardio-renal syndrome and chronic heart failure (CHF)

Cardiac magnetic resonance Imaging (MRI) for EF

EF can be determined using several invasive and non-invasive imaging modalities, either subjectively by visual estimation or objectively by quantitative methods. i.e., echocardiography, magnetic resonance imaging (MRI), computed tomography (CT), gated equilibrium radionuclide angiography (commonly referred to as multiple-gated acquisition [MUGA] scan) and gated myocardial perfusion imaging with either single-photon emission computed tomography (SPECT) or positron emission tomography (PET). In clinical setting, cardiac MRI and blood pool single-photon emission computed tomography are considered as gold standards for the assessment of LVEF *(2011. Nucl Med Commun. 32:121–128)* but have not found wide use for monitoring cardiac therapies in mice.

One of the early high-resolution MRI sequences for assessment of myocardial function and morphology in mice describes a cine performed with prospective ECG gating using a spoiled gradient echo technique and quantitative analysis using a semi-automated *approach (2007. J Nucl Med.48:288–294).* Indeed, MRI has been used for calculation of EF function in both healthy and MI-induced mice *(2006. J Nuc Med. 47:974–980),* in mice with permanent ischemic cardiomyopathy (ICM) or transient LAD ligation *(2009. J Nuc Med. 50:132–138),* and in different mouse models of cardiovascular diseases *(2012. EJNMMI Res. 2: 43-52)*

OBJECTIVE

The objective of this study is to evaluate the Tunac Arterial Plaque (TAP) mouse *(2017. J Clin Exp Cardiolog Suppl 8:1)* as a model for EF. Traditional mouse models involve genetically modified or surgically altered, whereas the TAP model is a wild mouse (C57Bl/6 strain) fed with high fat diet and treated with an environmental chemical pollutant (PCB) to mimic human lifestyle. Thus, the EF volume of treated and untreated mice will be measured per MRI as well as presence of arterial plaque.

MATERIALS AN METHODS

Mice

Twelve (12) ten-week-old male C57/Bl6 mice were obtained from Jackson Laboratories. High fat (60% fat) diet (D12451, DIO series diet, Opensource Diets) were given per experiment set-up below upon receipt. Animals were acclimated for 1 week and then 3 gavages of PCB administered every other day.

Group 1 mice – diet on regular chow
Group 2 mice – diet on regular chow + PCB
Group 3 mice – high fat diet (60% fat diet: DIO series, Opensource)
Group 4 mice (high fat + 3 PCB gavages)

Treatments

3,3',4,4'-Tetrachlorobiphenyl (PCB-77) was obtained from Neosyn Laboratories. The dry chemical was suspended in 15.22 ml of corn oil to deliver 200 µmol/kg in 0.2 ml by gavage per mouse according to the treatment schedule. All experiments were approved by the Henry Ford

Health System Institutional Animal Care and Use Committee. All reagents were acquired from Sigma-Aldrich (St. Louis, MO) unless otherwise stated.

Magnetic resonance imaging (MRI)

All studies were performed using a 7-Tesla Varian MRI system (Fig. 2).

Figure 2. A 7-Tesla Varian MRI system at the Henry Ford Health System laboratories

All animals received a baseline MRI scan that included a 3-plane localizer scan used to position the animal within the magnet.

This sequence was then followed by an intragate scan procedure that provided a series of 3 image sets that were used to align the heart to the proper orientation for a CINE scan (Motion sensitive MRI: A cine MRI is a special type of MRI image in which a series of static images are obtained at different times and then played back as a movie. Cine MRI is helpful in evaluating tissues that move such as the heart, flowing blood, or cerebral spinal fluid. It is occasionally used in evaluating bowel, joint or muscle motion.) that was used to estimate the ejection fraction. The final CINE scan that was referred to as a blackblood method that causes the blood to appear darker than the adjacent tissue. The CINE sequence required approximately 10 minutes and it acquires hundreds of images that are then sorted and reordered by the software. The resulting data set can then subsequently be run as a movie which is how we estimated the ejection fraction (EF), heart rate (HR) and respiratory rate (RR). The MRI protocol was as follows:

A. Ejection fraction imaging:

1. Run Localizer – position heart in center of magnet.

2. Planning 2: stack of axial images to localize blood vessels at the top of heart (9 slices), need to select level for either ejection fraction or aorta imaging.
3. Planning 3: coronal image set up for ejection fraction imaging using images from Planning 2: use to line up next image on 4 vessels at top of heart (produces an image along the long axis of the heart).
4. Planning 4: set up to produce a view that produces a 4-chamber heart image.

CINE_Blackblood_IG_FLASH: set up for CINE imaging: produces set of images showing the heart at various stages of the cardiac cycle, can be run as movie, this sequence provides the image data set that was used to estimate the cardiac ejection fraction.

B. Aorta & carotid artery imaging:

1. Technique involves multiple contrast weightings (e.g., T1, T2, and proton density). Localization of the correct plane angulation for the multislice experiments was planned from coronal and sagittal scout images.
2. Planning 3: set up for imaging of the aorta, using Planning 2 images to line up the slice on the aorta (produces an image showing the aortic arch, carotid and brachial arteries) run with at least 3 slices 0.5 mm thick).
3. Planning 4: use to set up for cross sectional imaging of aorta (FOV 20 mm, 3-5 slices, 0.5 mm thick) need to run 3 times with slices set to different angles ----- remember to copy geometry and save before running, watch that slice is not rotated too far or view may change.

The additional contrast enhanced scans were all performed after. Once the data are collected, they were transferred offline for processing. To estimate the ejection fraction, we used a program called Medviso Segment. After opening the data set and displaying the images in Segment, we used a command to auto detect end diastole and end systole. This provided the EF as a %. All animal groups were studied at multiple time points after treatment except for the two that received the HFD only.

Briefly, the heart is aligned to the proper orientation then an intragate scan is carried out for a CINE presentation (motion sensitive MRI in which a series of static images are obtained at various stages of the cardiac cycle and then played back as a movie). Particularly, the blackblood method (blood appears darker than the adjacent tissue) was used. The CINE sequence required approximately 10 minutes acquiring hundreds of images, sorted and reordered by a software program (Medviso Segment), which auto detect end diastole/end systole and calculate percent ejection fraction (EF), heart rate (HR) and respiratory rate (RR).

RESULTS:

General mouse health:

No mice died during the study, and no adverse effects were noted due to administration of PCB. No notable gross changes in weight, respiratory or heart rates attributable to the diet and PCB (Table1)

Table 1. Data on the experimental mice including weight, respiration, heart rate and % ejection fraction (EF%).

FileNam	PatientN	PatientID	Acquisit	Experim	Height[c	Weight[k	Sex	RespRa	HeartRa	R-R[ms	LVM[ml	LVM[g]	EDV[ml]	ESV[ml]	SV[ml]	EF[%]	CO[l/mir	PFR[ml	PER[ml
Bad data	JT01		2E+07	unable to estimate EF															
	JT01_010	JT01_010	2E+07	#6		0.027	O	82	422	133.33	0.0146	0.0153	0.0091	0.0029	0.0062	68.451	0.0028	0.1977	0.1993
	JT01A_0	JT01A-0	2E+07			0.029	O	80	429	133.33	0.0166	0.0174	0.012	0.0027	0.0093	77.591	0.0042	0.1978	0.3157
	JT02_11.	JT02	2E+07	#7		0.025	M	91	493	133.33	0.0139	0.0146	0.0134	0.0047	0.0087	64.738	0.0039	0.3301	0.22
	JT02A_(	JT02A-0	2E+07	#7		0.036	O	67	486	133.33	0.0194	0.0204	0.0132	0.0036	0.0096	72.583	0.0043	0.3418	0.2533
noisy	JT03_11.	JT03_HI	2E+07	#10		0.036	M	97	522	133.33	0.0143	0.015	0.0131	0.0047	0.0084	64.155	0.0038	0.3536	0.2789
	JT03-HF	JT03-HF	2E+07	#6		0.051	O	80	464	133.33	0.0187	0.0196	0.0141	0.0056	0.0085	60.338	0.0038	0.1022	0.2005
noisy	JT03-HF	JT03-HF	2E+07	#7		0.053	O	72	431	133.33	0.018	0.0189	0.015	0.0053	0.0097	64.538	0.0044	0.1844	0.4118
	JT03_HI	JT03_HI	2E+07	#5		0.053	O	62	394	133.33	0.018	0.0189	0.0153	0.0054	0.0099	64.74	0.0045	0.3449	0.1757
	JT04_11.	JT04_HI	2E+07	#8		0.03	M	95	532	133.33	0.0153	0.0161	0.0129	0.0038	0.0091	70.577	0.0041	0.2365	0.2095
	JT04-HF	JT04-HF	2E+07	#6		0.046	O	69	385	133.33	0.016	0.0168	0.0141	0.0056	0.0085	60.405	0.0038	0.2814	0.3111
	JT04-HF	JT04-HF	2E+07	#7		0.047	O	83	474	133.33	0.016	0.0168	0.0135	0.0057	0.0079	58.144	0.0035	0.1577	0.2163
	JT04-HF	JT04-HF	2E+07	#6		0.048	O	82	417	133.33	0.0168	0.0177	0.0135	0.0054	0.0081	59.948	0.0037	0.3111	0.19
	JT04-HF	JT04-HF	2E+07			0.046	O	71	430	133.33	0.0179	0.0188	0.0129	0.0054	0.0075	58.345	0.0034	0.2154	0.2054
	JT05_HI	JT05	2E+07			0.037	M	97	436	133.33	0.0157	0.0165	0.013	0.0043	0.0087	67.045	0.0039	0.2519	0.3043
	JT05_01	JT05_HI	2E+07	#7		0.047	O	96	445	133.33	0.0162	0.017	0.0168	0.0055	0.0112	67.085	0.0051	0.4941	0.3904
	JT05_01	JT05_HI	2E+07	#7		0.046	O	81	433	133.33	0.0173	0.0181	0.0116	0.0049	0.0067	57.991	0.003	0.2198	0.2172
	JT05-HF	JT05-HF	2E+07	#6		0.042	O	88	486	133.33	0.0162	0.017	0.013	0.0053	0.0077	59.1	0.0035	0.1277	0.31
	JT05-HF	JT05-HF	2E+07	#6		0.04	O	67	459	133.33	0.0323	0.0339	0.0275	0.0122	0.0153	55.648	0.0069	0.3152	0.455
	JT05_HI	JT05_HI	2E+07	#6		0.041	O	83	515	133.33	0.0166	0.0175	0.0132	0.0044	0.0088	66.471	0.0039	0.2362	0.2876
	JT05_HI	JT05_HI	2E+07			0.041	O			133.33	0.0163	0.0171	0.0134	0.0051	0.0083	61.761	0.0037	0.2045	0.1675
noisy	JT06_HI	JT06	2E+07	#8		0.034	M	92	457	133.33	0.0154	0.0162	0.013	0.0047	0.0082	63.501	0.0037	0.3881	0.1635
noisy	JT06_01	JT06_HI	2E+07	#7		0.043	O	93	444	133.33	0.0147	0.0155	0.0141	0.006	0.0081	57.56	0.0037	0.3454	0.1799
	JT06_01	JT06_HI	2E+07	#6		0.04	O	85	499	133.33	0.0154	0.0162	0.0118	0.0052	0.0066	56.221	0.003	0.2207	0.1563
	JT06-HF	JT06-HF	2E+07	#8		0.038	O	69	539	133.33	0.0161	0.0169	0.0128	0.0055	0.0072	56.56	0.0032	0.28	0.1814
	JT06-HF	JT06-HF	2E+07	#7		0.039	O	64	453	133.33	0.0173	0.0182	0.0137	0.0065	0.0072	52.564	0.0032	0.2136	0.1613
	JT07-HF	JT07-HF	2E+07	#6		0.049	O	81	396	133.33	0.0175	0.0184	0.0158	0.0057	0.0101	64.021	0.0046	0.2547	0.2201
Bad data	JT07_HI	JT07_HI	2E+07	#10		0.055	O	52	436	133.33	0.041	0.0431	0.027	0.0078	0.0193	71.288	0.0087	0.473	0.6542
	JT08-HF	JT08-HF	2E+07	#7		0.043	O	80	431	133.33	0.0172	0.0181	0.0136	0.0038	0.0098	72.291	0.0044	0.3196	0.2165
little nois	JT08_HI	JT08_HI	2E+07	#8		0.047	O	73	464	133.33	0.0171	0.018	0.0111	0.0043	0.0068	61.224	0.0031	0.3119	0.1655
	JT08_HI	JT08_HI	2E+07			0.047	O			133.33	0.0171	0.018	0.0111	0.0043	0.0068	61.224	0.0031	0.3119	0.1655
	JT09_01	JT09-HF	2E+07	#9		0.047	O	88	438	133.33	0.0163	0.0171	0.014	0.0053	0.0087	61.84	0.0039	0.1561	0.3281
noisy	JT10_01.	JT10-HF	2E+07	#7		0.045	O	90	442	133.33	0.0167	0.0176	0.013	0.0034	0.0096	73.622	0.0043	0.336	0.284

Ejection fraction percent:

Mice fed with normal diet showed normal ejection fraction volume (72%). Mice fed with normal diet then treated with PCB reduced EF% (68%) High fat diet alone without also effectively reduced EF% (63%), and the lowest reduction in EF were mice fed with high fat and PCB (61%), Fig. 2.

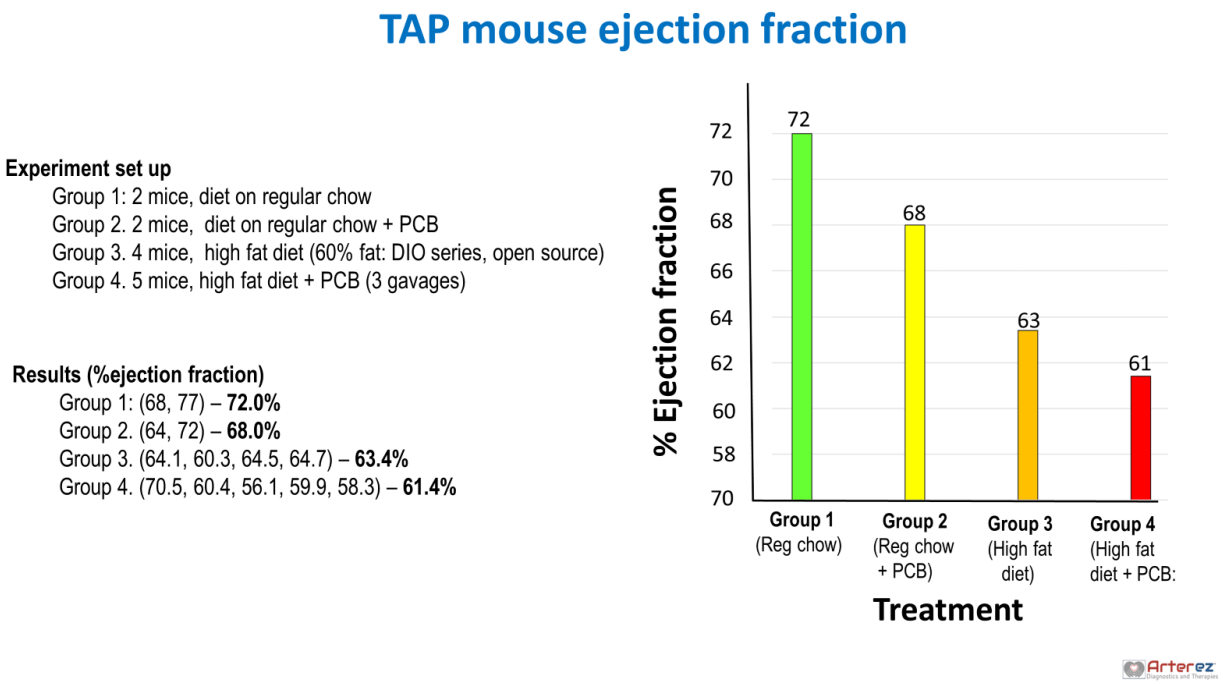

Figure 3. Ejection fraction profile in Tap mouse was most reduced when treated with high fat diet and PCB

*MRI imaging of aortal arch***.**
MR imaging of coronaries for plaques is impossible in mouse. The next option is MRI scan of the aortal arch. Indeed, MRI scan of mice in group 4 (high fat diet and PCB treatment) showed plaques in the aortal arch (Figs 4).

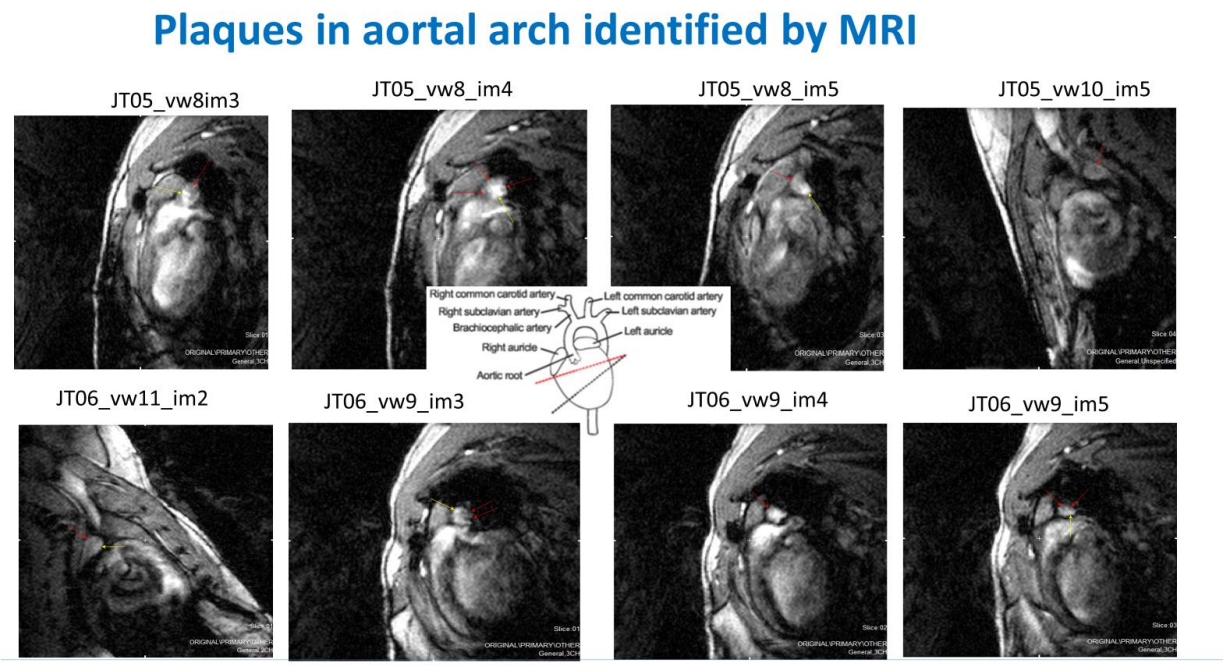

Figure 4. MRI scan of mice in group 4 (JT05, JT06) showing plaques in the aortal arch (red arrows)

DISCUSSION

Chronic diseases including arthritis, neurodegeneration, cancer, macular degeneration, cataract, autoimmune, adult respiratory syndrome, metabolic syndrome, diabetes and cardiovascular have complex etiologies that are triggered by lifestyle and environmental pollutants. Man-made chemical pollutants are part of the equation that triggers multifactorial diseases or xenopathic™ diseases. Pollutants are found in foods, beverages and packaging, clothes, cosmetics and cleaning products, furniture, paints, electronic equipment, plastics, and the list is long. Persistent pollutants including the lipophilic persistent organic pollutants (POPs) polychlorobiphenyls (PCBs) bio-accumulate in fatty tissues *(2009. Environ Health Perspect.117:417–25).* PCB was chosen for this study because they are the most ubiquitous environmental pollutant. PCBs are resistant to acids and bases as well as to heat, and have been used as an insulating material in electric equipment, such as transformers and capacitors, and also in heat transfer fluids and in lubricants, as plasticizers, surface coatings, inks, adhesives, flame-retardants, paints, and carbonless duplicating paper. Since 1929 around 2 million ton of PCBs have been produced, about 10% of which remain in the environment today *(2019. Science Direct 37: 399-407).* Pollutants disrupt certain signaling and differentiation pathways and to induce inflammation in the adipose tissue (*2007. Chemosphere 67:1463-7).* Pollutants and other blood debris trapped in a stagnant blood flow, due to high level of fat packaging lipoprotein (VLDL), triggers inflammation, disruption of endothelium, plaque formation and cardiovascular diseases (Fig 5)

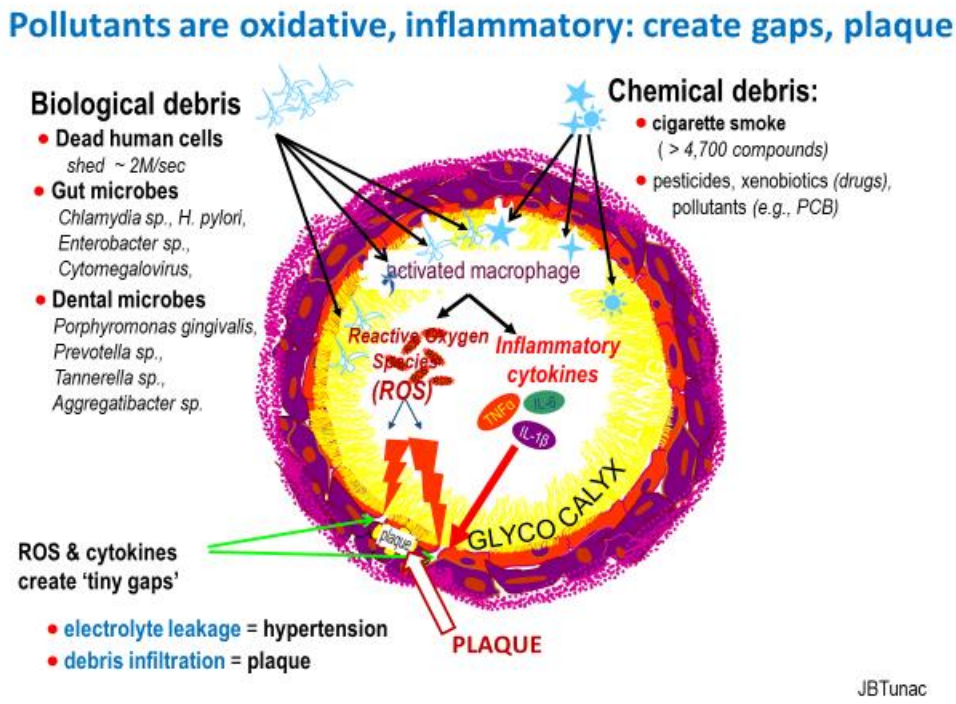

Figure 5. Biological and chemical pollutants in the arterial bends triggers inflammation, tiny endothelial gaps creating electrolyte leakage (hypertension) and debris infiltration (plaque)

Plaques stiffen myocytes or trigger apoptosis (2005. Cardiovascular Res 67: 21–29), disrupt pumping and reduced EFV (Fig 6)

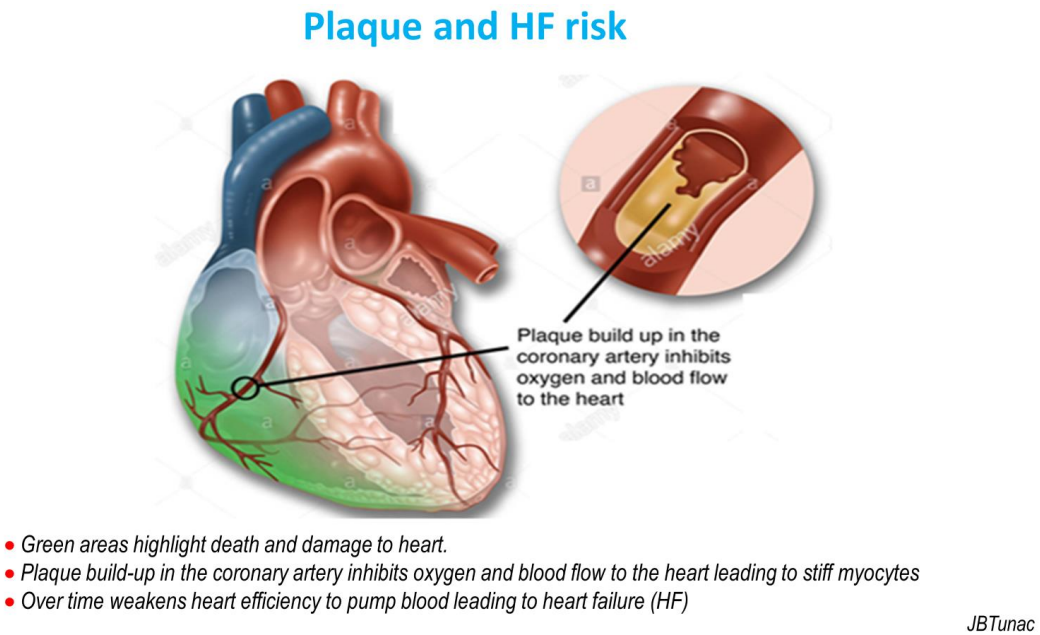

Figure 6. Green areas highlight death and damage to heart due to plaque, which stiffens heart myocyte and reduce ejection fraction (EF) volume.

While MRI has become a routine imaging to assess the myocardium in the clinic, coronary artery imaging offers challenges because of both their small caliber and complex motion. In animal models, MRI has been used to detect plaques in aortal arch *(2004. Arterios Thrombosis Vasc Biol 24:1714–1719).* Because, of the impossibility of scanning plaques in the coronaries of mice, detection of plaques in the aorta infers plaque formation in the coronaries. Moreover, our previous study where mice with high fat diet and PCB *(2017. J Clin Exp Cardiolog Suppl 8:1)* showed well-formed plaque formation in the brachiocephalic artery.

In summary, reduction in EFV starts with the disruption of the endothelial glycocalyx and the sequalae of cardiorenal syndrome. In a separate paper, repair of the glycocalyx lining and mitigating oxidative and inflammatory damages proved to effectively reverse and cure plaque in the TAP mouse model (unpublished).

FUTURE EXPERIMENT

Several drugs have been developed vs HF (Fig 7) but are palliative at best because they are symptom targeted. A sequel to this project will be to use the TAP model and evaluate Embotricin™ for its ability to restore the integrity of the arterial endothelial glycocalyx, reverse plaque formation and restore normal ejection fraction (EF) volume.

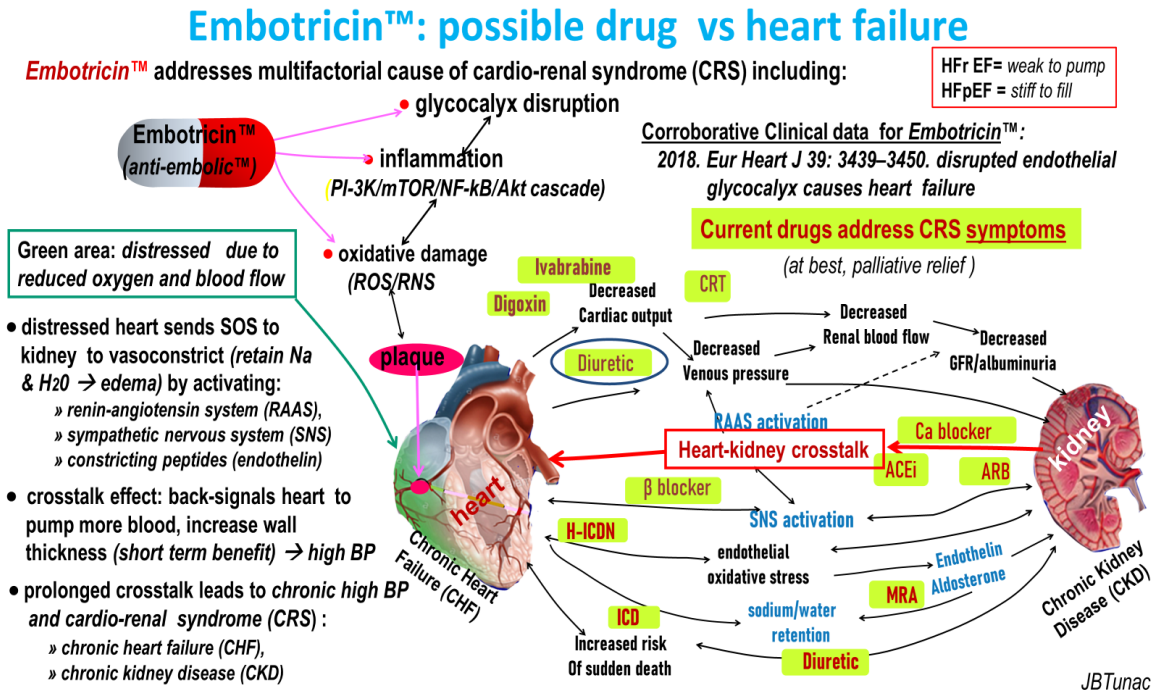

Figure 7. A compromised heart pumping result in reduced ejection fraction (EF) volume prompting heart kidney heart talk and a sequalae of diseases including heart failure (HF)